Bioorganic & Medicinal Chemistry 17 (2009) 3043–3052

Contents lists available at ScienceDirect

Bioorganic & Medicinal Chemistry

journal homepage: www.elsevier.com/locate/bmc

Synthesis, cytotoxic and combined cDDP activity of new stable curcumin derivatives

Erika Ferrari [a], Sandra Lazzari [a], Gaetano Marverti [b], Francesca Pignedoli [a], Ferdinando Spagnolo [a], Monica Saladini [a,*]

[a] Department of Chemistry, University of Modena and Reggio Emilia, Via Campi 183, 41100 Modena, Italy
[b] Department of Biomedical Science, University of Modena and Reggio Emilia, Via Campi 287, 41100 Modena, Italy

ARTICLE INFO

Article history:
Received 12 November 2008
Revised 24 February 2009
Accepted 7 March 2009
Available online 14 March 2009

Keywords:
Curcuminoidic compounds
Cytotoxicity
Kinetic stability
Metal complexes
Cisplatin
Ovarian carcinoma
Vero cells

ABSTRACT

New curcumin derivatives are synthesized in order to improve chemical properties of curcumin. The aromatic ring glycosylation of curcumin provides more water-soluble compounds with a greater kinetic stability which is a fundamental feature for drug bioavailability. The glycosylation reaction is quite simple, low cost, with high yield and minimum waste. NMR data show that the ability of curcumin to coordinate metal ion, in particular Ga(III), is maintained in the synthesized products. Although the binding of glucose to curcumin reduces the cytotoxicity of the derivatives towards cisplatin (cDDP)-sensitive and -resistant human ovarian carcinoma cell lines, the compounds display a good selectivity since they are much less toxic against non-tumourigenic Vero cells. The combination of cDDP with the most active glycosyl-curcuminoid drug against both cDDP-sensitive and -resistant as well as against Vero cell lines is tested. The results show an improvement of cDDP efficacy with higher selectivity towards cancer cells than non-cancer cells. These studies indicate the need for developing new valid components of drug treatment protocols to cDDP-resistant cells as well.

1. Introduction

Cisplatin (cDDP) is a compound in clinical use for the treatment of malignancies of the urogenital tract and other cancers.[1] The overall clinical success of chemotherapy with cDDP is complicated by toxicity and diminished by intrinsic and acquired tumour resistance to this drug. cDDP-resistance is multifactorial and involves decreased drug accumulation, increased glutathione and metallothioneines content and enhanced DNA repair activity.[2] The development of new chemotherapeutic agents and new combination regimen is thus highly desirable.

Curcumin [1,7-bis(3-hydroxy-4-methoxyphenyl)hepta-1,6-diene-3,5-dione] is a well-known dietary pigment derived from *Curcuma longa L.* It has been shown to inhibit growth of several types of malignant cells both in vivo and in vitro, various mechanisms of action have been proposed which may be correct.[3] Recent studies demonstrated that curcumin is also able to reduce the proliferation of human ovarian carcinoma cells with potency comparable to cisplatin[4] by inducing G_2/M phase cell-cycle arrest.[5]

Moreover curcumin demonstrated a great ability in chelating essential metal ions such as Cu(II)[6] and these complexes showed to possess higher ROS scavenging ability than curcumin.[7] Previous investigation assessed the ability of curcumin to form stable complexes with a fundamental metal ion such as Fe^{3+},[8] and iron chelation was related to biological activity of curcumin.[9] Since tumour cells growth requires higher iron level, iron chelators are used as antitumour therapies.[10] Due to its excellent pharmacodynamic profile, curcumin proceeded onto clinical trials however its use is limited by a poor bioavailability.[11] The main drawbacks in the clinical use of curcumin are: low solubility, high rate of metabolism, inactivity of metabolic products and/or rapid elimination from the body. In order to improve curcumin water solubility and drug-delivery, different approaches have been reported such as curcumin conjugation with nucleosides[12] and biopolymers.[13,14]

This paper reports a simple synthetic pathway able to give new glycosyl curcuminoids (Scheme 1) with high yield and low reaction time; the compounds are completely characterized. The chemical stability of synthesized compounds is also evaluated and compared with curcumin as kinetic stability is an important factor that influences serum level of active molecules. ^{1}H NMR and UV–vis spectroscopy are here used to evaluate metal chelating ability of studied compounds.

These curcumin derivatives are tested against a cDDP-sensitive human ovarian carcinoma cell line, 2008 cells, and its -resistant counterpart, C13* cells.

* Corresponding author. Tel.: +39 0592055040; fax: +39 059373543.
E-mail addresses: gaetano.marverti@unimore.it (G. Marverti), monica.saladini@unimore.it (M. Saladini).

0968-0896/$ - see front matter © 2009 Elsevier Ltd. All rights reserved.
doi:10.1016/j.bmc.2009.03.016

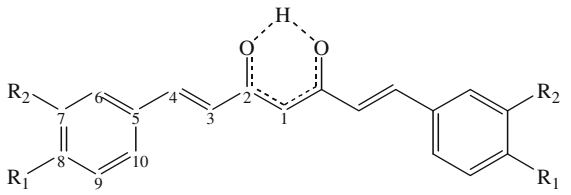

Compound	R_1	R_2
5	OH	OCH_3
6	OAc	OCH_3
7	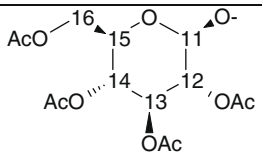 (AcGlcO-)	H
8	AcGlcO-	OH
9	AcGlcO-	OCH_3
10	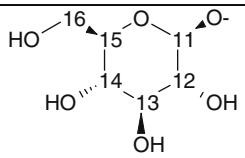 (GlcO-)	H
11	GlcO-	OH
12	GlcO-	OCH_3

Scheme 1.

A fundamental requisite for the clinical efficacy of anticancer drugs is selectivity of action, that means a good therapeutic index, therefore it would be helpful to test cytotoxic activity of these curcumin derivatives towards normal cell line. In the present study, the antitumour activity of the compounds has been tested in parallel with the investigation of the possible changes in growth and cell proliferation patterns induced by these curcumin analogs on Vero cells, an immortal, non-tumourigenic fibroblastic cell line.[15,16] It is well known that curcumin has a antiproliferative effect both on ovarian cancer cells and fibroblast cells, although it induces different phase cell-cycle arrest.[5,17] Even if the Vero cell lineage is obtained from a different species (African green monkey kidney), it shares a common embryonic origin (mesoderm) with cells from human genital tract.[18] Vero cells are usually considered as control cells[19] as they present very well defined properties which allow to easily observe possible growth modification by chemical agents. In addition, this line is non-tumourigenic but immortalized, allowing to culture cells for longer than normal cell line.

2. Results and discussion

2.1. Chemistry

Existing reports detail the synthesis of compound **12**,[20] however the low yield and the formation of a mixture of glycosilated products suggested to try a new synthetic pathway extensible to all glycosilated derivatives.

The S_N2 reaction of 3-substituted 4-hydroxyl-benzaldehyde on 2,3,4,6-tetracetyl-α-D-glucopyranosyl bromide (**1**) is performed by activation of phenolic moiety using an aqueous NaOH solution; the glycosylated products (**2–4**) are well recrystallised by EtOH and only β-anomer is detected. The reactivity of 3,4-dihydroxyl-benzaldehyde and vanillin with respect to 4-hydroxyl-benzaldehyde is due to the electron withdrawing effect of *meta*-substituent. Therefore the increasing phenolic acidity activates the phenolate ion in the SN reaction, overcoming the steric hindrance of the vicinal substituent.

The general synthesis for curcumin analogs is shown in Scheme 2. The new synthetic pathway represents an improvement of Pabon reaction[21] as it concerns yield, reaction time, costs and waste.

Boric anhydride is added to form a complex with 2,4-pentanedione (acac) in order to protect C-1 from Knoevenagel condensation and lead to aldol condensation. The proper solvent is DMF, which is able to provide high solubility for both reactants and intermediates together with a medium of suitable polarity for the process. DMF also facilitates the isolation and separation of the curcuminoids (**5**–**9**) from by-products.

Due to depletion of diketone by side reactions, the 1,8/1 benzaldehyde/diketone stoichiometric ratio is preferred and *n*-butylamine was chosen as condensation catalyst.

During the reaction, water is produced upon formation of the acac complex as well as upon formation of curcuminoid itself. Since water can generate side reactions and substantially reduce the yield, the reaction is carried out under anhydrous conditions, and tributylborate $(n\text{BuO})_3\text{B}$ is added as drying agent.

The pure products separate from reaction mixture and NMR data support a purity greater than 98%, therefore no chromatographic purification is needed. This one pot reaction is characterized by quite good yields (~80%), short time (6 h) and small volumes of implied solvents (1 ml of DMF for 0.5 mmol of product).

The final deacetylation step to obtain compound **10**–**12**, performed by use of CH_3ONa, is a quantitative reaction and no problems of decomposition are observed for all the products.

2.2. NMR spectroscopy

Fe-sequestering ability is often connected to drugs anticancer activity[22] therefore we tested metal affinity of curcumin deriva-

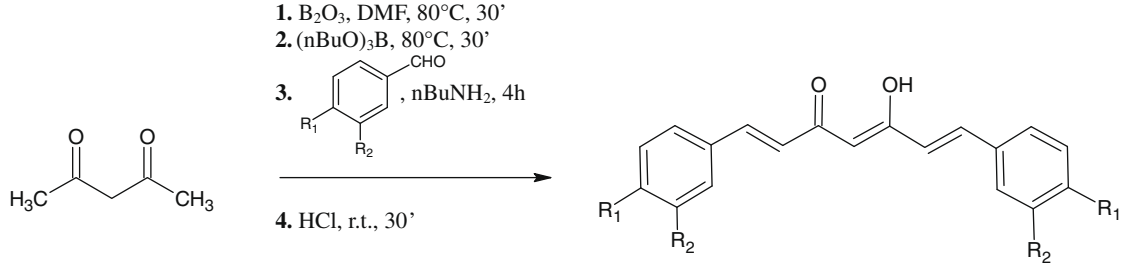

Scheme 2.

tives by means of NMR technique which provides useful information on coordination sites and complexes stoichiometry.

All the molecules show a typical spectral pattern of a keto-enolic moiety,[8,23] the enolic proton is mobile in fast exchange with residual HOD and implied in a strong intra-molecular hydrogen bond that makes it equally shared by the two oxygen atoms as confirmed by crystal structure of analogous compounds.[24] The ability to chelate metal ions is tested by adding $Ga(NO_3)_3$ to a solution of the ligand; diamagnetic Ga(III) is used as NMR probe instead of paramagnetic Fe(III).[25,26]

The addition of $Ga(NO_3)_3$ in 1/2 metal to ligand Me/L molar ratio to a solution of compounds **10**, **11**, **12** (Scheme 1), at acidic pH, immediately originates new signals, in slow chemical exchange in NMR time scale, whose spectral pattern resembles the one of the free ligand but strongly downfield shifted (Fig. 2, Tables 1 and 2). Since little reductions are observed in the pH value (~0.5 pH units), the formation of the new sets of signals is not a consequence of the decreased pH induced by Ga(III) hydrolysis but is more reasonably attributed to the formation of a complex species with a 1/2 Me/L molar ratio. The greatest downfield shift is for the H-4 signal; H-4 probably 'feels' the delocalized positive charge of the complex originated from metal chelation by keto-enolic moiety. In line with the behaviour of curcumin,[8] the phenolic group of **11** does not interact with the metal ion. Small changes for the aromatic protons are due to delocalization of the metal charge along the aliphatic chain and aromatic rings. As more Ga(III) is added a new downfield species appears hinting the formation of another complex species characterized by 1/1 Me/L molar ratio, independently on the ligand. No evidence of an interaction between sugar moiety and metal ion is observed by NMR spectroscopy in acid media, although we cannot exclude a possible glycoside interaction with the metal ion under physiological conditions, as reported in literature in the solid state.[27–29]

2.3. UV–vis spectroscopy

Similarly to curcumin, glucosyl curcuminoids maintain their dye properties showing a absorbance maximum in the 300–400 nm spectral range. By adding Ga(III) solution to the free ligands in acidic condition (pH ~ 4.5) a general blue shift is observed due to the interaction between the metal ion and the keto-enolic moiety, Figure 1 reports gallium titration of **12** at λ = 480 nm the

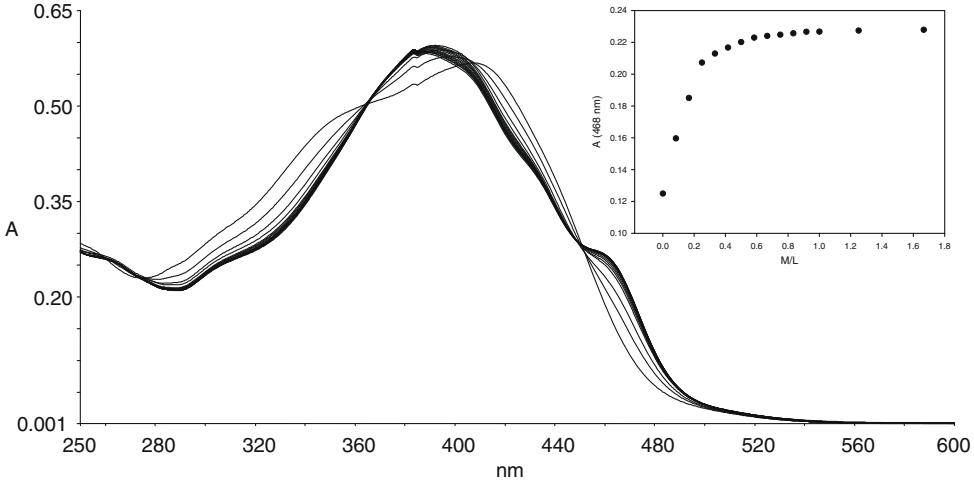

Figure 1. Spectrophotometric titration of **12** (2.5×10^{-5} M) with $Ga(NO_3)_3$ in aqueous solution. The inset shows the plot of absorbance versus metal to ligand molar ratio (Me/L) at λ = 480 nm.

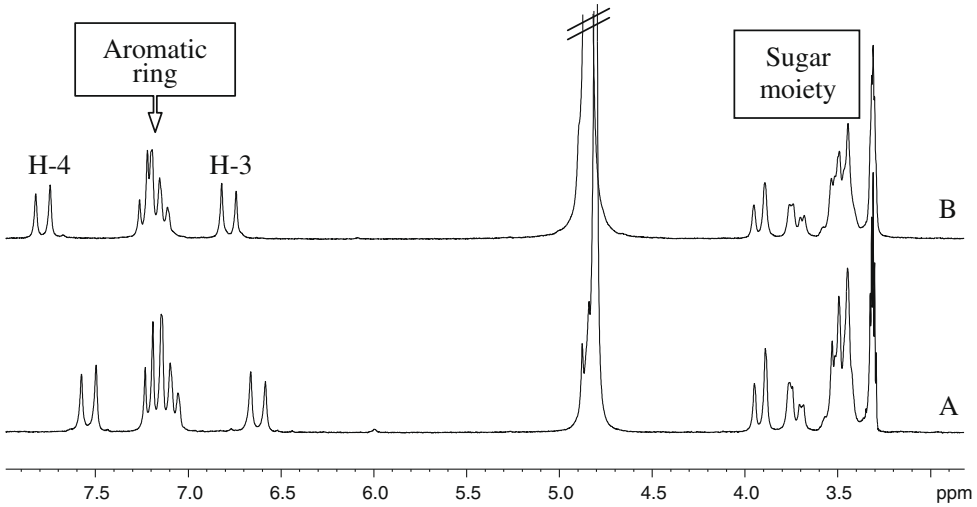

Figure 2. ^{1}H NMR spectra of compound **11** (A) and **11**/$Ga(NO_3)_3$ 2:1 molar ratio system (B) in CD_3OD.

Table 1
^{1}H chemical shifts (δ ppm) of ligands, their gallium(III) complexes and $\Delta\delta$ ($\delta_{complex} - \delta_{ligand}$) registered at 300 K in CD_3OD

	H-1	H-3	H-4	H-6	H-7	H-9	H-10
Compound **10**	6.01	6.69	7.62	7.6	7.14	7.14	7.6
Me/L 1:2	6.06 (0.05)	6.83 (0.14)	7.80 (0.18)	7.62 (0.02)	7.16 (0.02)	7.16 (0.02)	7.62 (0.02)
Me/L 1:1	6.13 (0.12)	6.87 (0.18)	7.88 (0.26)	7.67 (0.07)	7.19 (0.05)	7.19 (0.05)	7.67 (0.07)
Compound **11**	6.03	6.65	7.57	7.17	—	7.24	7.10
Me/L 1:2	6.04 (0.01)	6.76 (0.11)	7.72 (0.15)	7.17 (0.00)		7.22 (−0.02)	7.09 (−0.01)
Me/L 1:1	6.12 (0.09)	6.81 (0.16)	7.81 (0.24)	7.22 (0.05)		7.27 (0.03)	7.16 (0.06)
Compound **12**	6.02	6.72	7.60	7.12	—	7.18	7.18
Me/L 1:2	6.04 (0.02)	6.84 (0.12)	7.76 (0.16)	7.15 (0.03)		7.17 (−0.01)	7.16 (−0.02)
Me/L 1:1	6.13 (0.11)	6.90 (0.18)	7.86 (0.26)	7.18 (0.06)		7.23 (0.05)	7.25 (0.07)

Table 2
^{13}C chemical shifts (δ ppm) of ligands, their gallium(III) complexes and $\Delta\delta$ ($\delta_{complex} - \delta_{ligand}$) registered at 300 K in CD_3OD

	C-1	C-2	C-3	C-4	C-5	C-6	C-7	C-8	C-9	C-10
Compound **10**	102.8	185.6	124.5	142.1	131.6	131.6	118.9	161.6	118.9	131.6
Me/L 1:2	102.7 (−0.1)	186.8 (1.2)	126.7 (2.2)	143.6 (1.5)	131.5 (−0.1)	131.9 (0.3)	119.0 (0.1)	161.8 (0.2)	119.0 (0.1)	131.9 (0.3)
Me/L 1:1		186.8 (1.2)	125.5 (1.0)	144.8 (2.7)	132.0 (0.4)	131.8 (0.2)	118.6 (−0.3)	162.1 (0.5)	118.6 (−0.3)	131.8 (0.2)
Compound **11**	102.8	185.4	124.5	142.1	132.6	116.2	147.7	149.4	118.8	122.8
Me/L 1:2	104.3 (1.5)	186.5 (1.1)	126.7 (2.2)	143.4 (1.3)	132.6 (0.0)	116.9 (0.7)	148.3 (0.6)	149.4 (0.0)	118.8 (0.0)	123.4 (0.6)
Me/L 1:1		186.8 (1.4)	126.3 (1.8)	144.5 (2.4)	132.5 (−0.1)	117.2 (1.0)	149.6 (1.9)	150.2 (0.8)	119.0 (0.2)	123.7 (0.9)
Compound **12**	102.8	185.6	124.5	142.1	132.1	112.1	149.6	150.1	117.3	122.5
Me/L 1:2	103.6 (0.8)	186.8 (1.2)	126.8 (2.3)	143.5 (1.4)	132.2 (0.1)	112.6 (0.5)	150.1 (0.5)	150.2 (0.1)	117.3 (0.0)	122.8 (0.3)
Me/L 1:1		186.9 (1.3)	126.3 (1.8)	145.0 (2.9)	132.0 (−0.1)	112.8 (0.7)	150.8 (1.2)	150.8 (0.7)	117.2 (−0.1)	122.8 (0.3)

absorbance increases with Me/L molar ratio reaching a maximum at Me/L value of 0.5 corresponding to a ML_2 complex, confirming NMR data (insert Fig. 1).

2.4. Kinetic study

Chemical stability is a fundamental drug feature therefore we studied the degradation process of our compounds following the time dependent diminishing in UV–vis λ max absorbance. By plotting $\ln(A_t/A_0)$ versus time at 37 °C and constant ionic strength a linear regression for all the compounds is observed hinting a first order kinetic process. Figure 3 shows that degradation is extremely slow at pH 7 for all glycosylated compounds (**10**, **11** and **12**) being the percentage of decomposed compounds less than 30% during the first hour, while curcumin is 50% decomposed in the same experimental conditions; previous study reported that curcumin is almost completely decomposed after 1 h.[30] The presence of sugar moiety delays degradation processes being the $t_{1/2,}$ estimated from curves in Figure 2, in the range 150–200 h, resembling the stability of cyclodextrin complexed curcumin ($t_{1/2}$ >100 h).[31] If compared to curcumin the presence of acetyl groups in compound **6** also increases kinetic stability (4% decomposed after 1 h) suggesting that the fast degradation of curcumin is strongly influenced by phenolic groups. The kinetic stability of curcumin derivatives is also confirmed by NMR data. In fact no relevant changes in ^{1}H chemical shifts and integrated areas are observed during the first 72 h. The nature of *meta*-substituent does not drive the degradation process in glycosylated products, although compound **10** is the more stable one during the first 2 h.

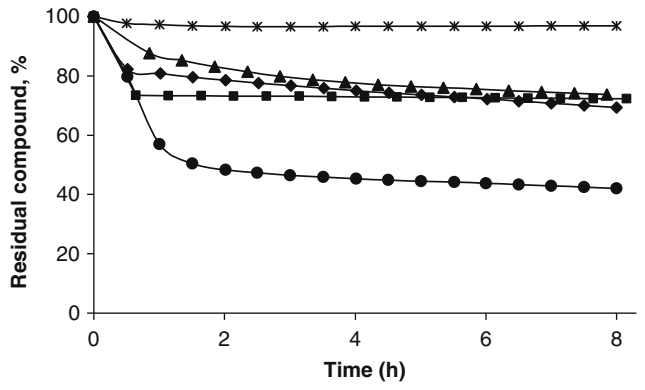

Figure 3. Plotting of residual compound percentage versus time (h) for compounds: **5** (●), **6** (*), **10** (▲), **11** (♦), **12** (■). Spectrophotometric measurements were performed in buffer solution (pH 7) at 37 °C.

2.5. Cytotoxic assay

In order to compare the growth inhibitory effects of curcumin and its derived drugs, we tested the cytotoxicity of curcumin against a cDDP-sensitive human ovarian carcinoma cell line and its acquired cDDP-resistant counterpart. cDDP-resistant cell line shows a 3.4-fold cross-resistance to curcumin, since its IC_{50} value (IC_{50} = drug concentration that reduces cell growth by 50%) is 17 ± 1 μM in C13* cells and 5.0 ± 0.4 μM in 2008 cells. At 10 μM curcumin inhibits 2008 cell growth at 90% while cDDP-resistant cells still survive to this concentration by a nearly 60% and display a more dose-related sensitivity to the compound than the parental line (data not shown). According to the reports of Adams et al.,[32]

Table 3
IC_{50} values deduced from the dose–response curves in 2008 and C13* cells

Compounds	Cell lines (IC_{50}, μM)		RF^I	Vero cell	RF^{II}
	2008 cells	C13* cells			
Curcumin	5.0 ± 0.4	17 ± 1	3.4	22	1.3
6	9.8 ± 0.8	40 ± 3.7	4.1	45	1.1
10	22 ± 1.9	83 ± 7	3.8	330	3.97
11	480 ± 37	ND	>2	ND*	
12	220 ± 16	840 ± 68	3.8	ND*	
cDDP	1.5 ± 0.1	18.4 ± 1.6	12.3	10	

Resistant factors: RF^I = IC_{50} resistant/IC_{50} parent line, RF^{II} = IC_{50} Vero cell/ IC_{50} resistant. (*ND = not determined).

curcumin cytotoxicity against the cell model of our study is also confirmed to be comparable to that of cDDP, as reported in Table 3. Five micromolar curcumin concentration (IC_{50} value in 2008 cells) blocks Vero cell growth by only 10%. Ten micromolar curcumin concentration inhibits 2008 and C13* cell growth by about 90% and 45%, respectively and decreases Vero cell proliferation by about 25% (data not shown).

Figure 4 shows the cytotoxicity of compounds **6**, **10**, **11**, **12**, in 2008 and C13* cells, and Table 3 reports the corresponding IC_{50} values.

The acetylation of the phenolic groups of curcumin provides compound **6**, whose cytotoxicity (Fig. 4, panel A) is almost reverted to that of curcumin, being compound **6** only twofold less potent than the lead compound. As a result, the IC_{50} values of **6** are 9.8 ± 0.8 μM and 40 ± 4 μM in 2008 and in C13* cells, respectively. The dose–response curve of cell survival to **6** shows a plateau from 20 μM to higher concentrations only for 2008 cells. This response trend is very similar to that shown by the same cells treated with curcumin. In addition, the twofold lower effectiveness of **6** with comparison to curcumin is also maintained against Vero cells, whose growth is 50% inhibited by 45 ± 5 μM **6** (Fig. 5) and 22 ± 2 μM curcumin (data not shown).

With the purpose to improve curcumin water-solubility the phenyl groups have been functionalized with glucose in position 4, obtaining compound **12**. As shown in Figure 4 (panel D), compound **12** is a less potent inhibitor than curcumin against either 2008 and C13* cell growth. After 72 h-exposure the IC_{50} values obtained were 220 ± 16 μM and 840 ± 68 μM, respectively; thus displaying a 3.8-fold cross-resistance to the analogue in C13* cells. Cell growth inhibition of **12** is accompanied with a very scant cytotoxicity against the non-neoplastic monkey fibroblasts (Fig. 5), whose growth is inhibited by a maximum of 20% even up to 750 μM.

To increase the antitumour activity of glycosyl derivatives in comparison to curcumin, we have replaced methoxyl groups in position 3 with hydroxylic group, producing compound **11**. Figure 4 (panel C) shows that cDDP-sensitive cells are also more responsive

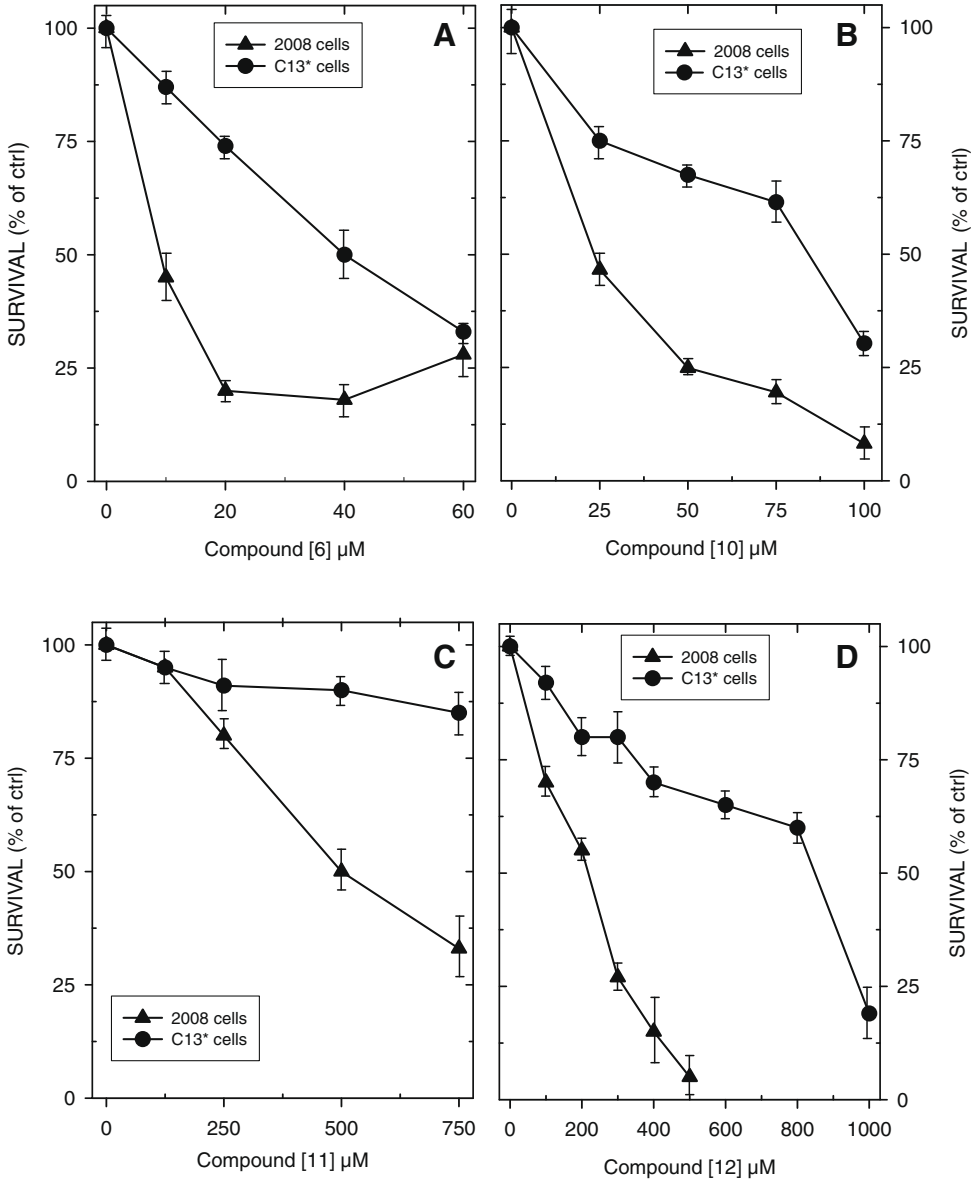

Figure 4. Cytotoxicity of β-diketones in 2008 (○) and C13* (●) cells. 24 h after seeding, cells were exposed for 3 days to the indicated concentrations of the drugs and then cytotoxicity was assessed by the crystal violet method. Results represent the mean of three separate experiments performed in duplicate. The standard error was within ±10% for each data point.

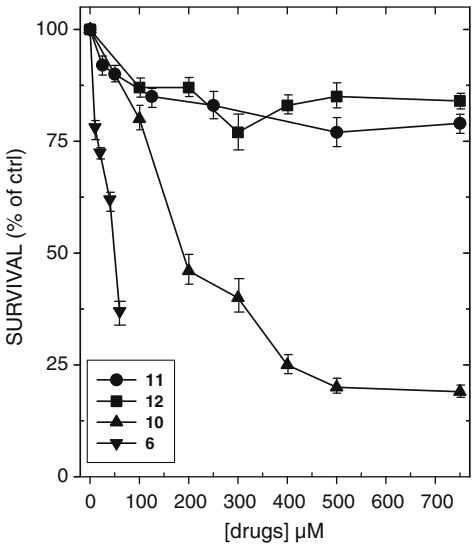

Figure 5. Dose–response effects of the β-diketones on growth of Vero cells. 24 h after seeding, cells were exposed for 3 days to the indicated concentrations of the drugs and then cytotoxicity was assessed by the crystal violet method. Results represent the mean of three separate experiments performed in duplicate. The standard error was within ±10% for each data point.

to **11** than their resistant counterpart. While the IC_{50} value of **11** is about 500 μM in 2008 cells, in C13* cells was not possible to obtain the IC_{50} value in the concentration range investigated. At 750 μM, 2008 and C13* cells are inhibited by 70% and only 15%, respectively. However, the cytotoxicity of **11** against C13* cells parallels a poor inhibition of Vero cell growth, which survive by nearly 80 % up to 750 μM **11** (Fig. 5).

The elimination of *meta*-substituent on the phenyl ring gives compound 10. Figure 4 (panel B) provides evidence that this removal is actually effective since the IC_{50} values are 10-fold decreased both in 2008 and in C13* cells (Table 3), when compared to **12** compound. Again, C13* cells are also 3.8-fold cross-resistant to **10**, as deduced from IC_{50} values and resistant factor RF^{I} ($RF^{I} = IC_{50}$ resistant/IC_{50} parent line) reported in Table 3. Compound **10** displays a good selectivity since it is 15- and 4-fold less toxic against Vero cells (IC_{50} value 330 ± 31 μM) than against 2008 and C13* cells, respectively (Fig. 5). The resistant factor RF^{II} value ($RF^{II} = IC_{50}$ Vero cell/ IC_{50} resistant) (Table 1) shows a better selectivity of **10** towards C13* cells than against Vero cells when compared to curcumin and compound **6**, indicating that even cDDP-resistant cells are somehow more responsive to the derivative than control non-tumourigenic line.

These data suggest that binding a glucose molecule to curcumin greatly reduces the cytotoxicity of the derivatives, as indicated by the increased values of IC_{50} both in sensitive and resistant cell lines. This diminished effectiveness could be ascribed to the greater molecular complexity and bulkiness compared to curcumin, which may limit cellular penetration of the compounds. According to this hypothesis the replacement of glucose with acetoxy group restores the cytotoxicity almost to the level of curcumin, being the related IC_{50} value about only doubled with respect to the lead molecule. The growth-inhibitory activity increases by decreasing the electron withdrawing effect of *meta*-substituent, as indicated by the sequence of potency **11** < **12** < **10**. The absence of *meta*-substituents on the aromatic ring may facilitate the electron conjugation and delocalization on the sp^2 moiety, which may be responsible of the enhanced cytotoxicity observed in both lines.

Cisplatin (cDDP) is frequently used in combination with other drugs in order to minimize the side-effects of each compound. Recently it has been shown that curcumin treatment improved the efficacy of cDDP-based chemotherapy against human laryngeal carcinoma cells.[33]

In this regard we have tested the combination of cDDP with the most active drug among glycosyl-curcuminoids, **10**, against both sensitive and resistant cell lines. The nature of the drug interaction between cDDP and **10** is investigated by median-effect analysis, according to Chou and Talalay,[34] which calculates the combination indexes (CI), a measure of drug interaction effect. A CI <1 indicates synergism, CI = 1 additivity and CI >1 antagonism. Compound **10** and cDDP were combined at a ratio of 20:1 for 2008 cells and 5:1 for C13* cells. Scheduling experiments were carried out by adding both agents either simultaneously or sequentially to determine the optimum conditions. As shown in Figure 6 the concurrent drug treatment schedule appears to be the most effective combination against 2008 cell line, being the CI values always lower than 1 (panel A). Sequential combinations do not improve the interactive effects of the drugs since a 24 h-pretreatment with **10** causes, at most, supra-additive effects with 2 combinations and slight synergistic inhibition with 5 μM cDDP (panel E). In addition, when cDDP was added 24 h before **10**, antagonistic interactions is observed with all combinations tested (panel C).

All treatment schedules with the two drugs bring about similar interactive positive effects against the resistant line; in fact, almost additive effects at 5 and 10 μM cDDP and synergistic cell killing at 20 μM are displayed. In particular, the lowest CI (0.35), indicative of a strong synergy, is observed when **10** is combined concurrently with 20 μM cDDP (panel B). These results indicate that **10** may improve the efficacy of cDDP in the sensitive line more than in the resistant line. On the contrary, **10** post-treatment cause a detrimental effect on cDDP action. Despite their resistance to each drug alone, C13* cell growth could be successfully inhibited by the appropriate combinations of the two drugs.

In all the schedules tested, the interactive effects of the two drugs resulted highly antagonistic against the non-tumourigenic lineage, Vero cells (Fig. 7). As it appears, antagonism of the combinations increases with cDDP concentrations, reaching very high CI values at the doses of cDDP used in C13* cells. These data indicate the selectivity of the interactive effects of cDDP with **10** that, when properly combined, might be more potent inhibitors against carcinoma cells than against non-tumourigenic control cells.

3. Conclusion

The curcumin derivatives are easily synthesized with high yield and low costs; they demonstrate a greater kinetic stability if compared to curcumin, maintaining the metal-ligating ability through β-diketo moiety. Among curcumin derivatives compound **6** and **10** demonstrated the better cytotoxicity towards 2008 and C13* cell lines. In particular compound **10** displays a good selectivity since it is much less toxic against non-tumourigenic Vero cells. Compound **10** improves also the efficacy of cDDP in sensitive cell line and also in resistant cell line while the combination of the two drugs is highly antagonistic against non-tumourigenic cell line indicating an improved selectivity.

4. Experimental

4.1. Synthesis

4.1.1. 2,3,4,6-Tetracetyl-α-D-glucopyranosyl bromide (1)

Compound **1** was synthesized quantitatively by reaction of 1,2,3,4,6-pentaacetyl-β-D-glucopyranose with HBr 30% in glacial acetic acid, at room temperature for 4 h.[35]

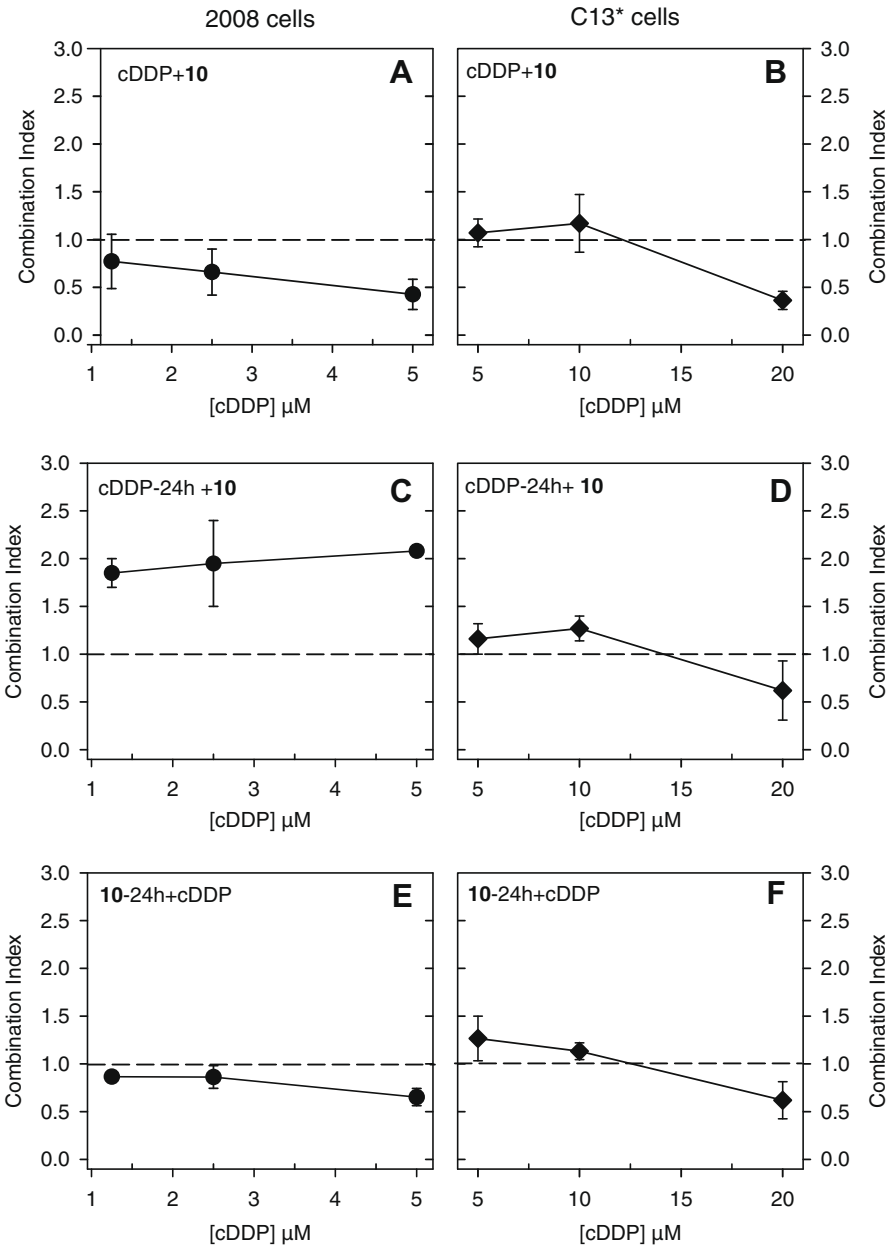

Figure 6. Median-effect analysis of cisplatin combined with compound **10** at the constant ratio of 1:20 for the 2008 cells (left panels) and of 1:5 for the C13* cells (right panels). Cells were allowed to attach overnight and then simultaneously (upper panels) or sequentially (middle and lower panels) treated with **10** and with the indicated concentrations of cDDP in 24-well plates. Following a 3-day exposure, cells were stained with crystal violet. Results are expressed as combination indexes (CI), where CI <1 indicate synergistic effects, CI >1 indicate antagonistic effects, CI = 1 indicate additivity. Results represent the mean of three separate experiments performed in duplicate. The standard error was within ±10% for each data point.

4.1.2. 4-(2,3,4,6-Tetracetyl-β-D-glucopyranos-1-yloxy)benzaldehyde (2); 3-hydroxy-4-(2,3,4,6-tetracetyl-β-D-glucopyranos-1-yloxy)benzaldehyde (3); 3-methoxy-4-(2,3,4,6-tetracetyl-β-D-glucopyranos-1-yloxy)benzaldehyde (4)

The appropriate benzaldehyde were solubilized in NaOH, and then slowly dropped in an equimolar solution of 1 in acetone. The reaction was kept under stirring overnight at room temperature, and a precipitate splits up when water was added. The isolated product was recrystallized from EtOH. Anal. Calcd for $C_{21}H_{23}O_{11}$ (**2**): C, 55.83; H, 5.14. Found: C, 56.02; H, 5.52, yield 80%; Anal. Calcd for $C_{21}H_{23}O_{12}$ (**3**): C, 53.91; H, 4.96. Found: C, 54.22; H, 4.28, yield 85%; Anal. Calcd for $C_{22}H_{25}O_{12}$ (**4**): C, 54.84; H, 5.23. Found: C, 55.22; H, 5.82, yield 80%; NMR chemical shifts (ppm in $CDCl_3$): (**2**) H-11 5.31, H-12 5.21, H-13 5.30, H-14 5.17, H-15 3.92, H-16 4.28, H-16′ 4.18, H-6 7.85, H-7 7.10, H-9 7.10, H-10 7.85; (**3**) H-11 5.08, H-12 5.29, H-13 5.36, H-14 5.17, H-15 3.92, H-16 4.32, H-16′ 4.20, H-6 7.46, H-9 7.08, H-10 7.40; (**4**) H-11 5.31, H-12 5.11, H-13 5.31, H-14 5.17, H-15 3.84, H-16 4.27, H-16′ 4.19, H-6 7.43, H-9 7.21, H-10 7.41.

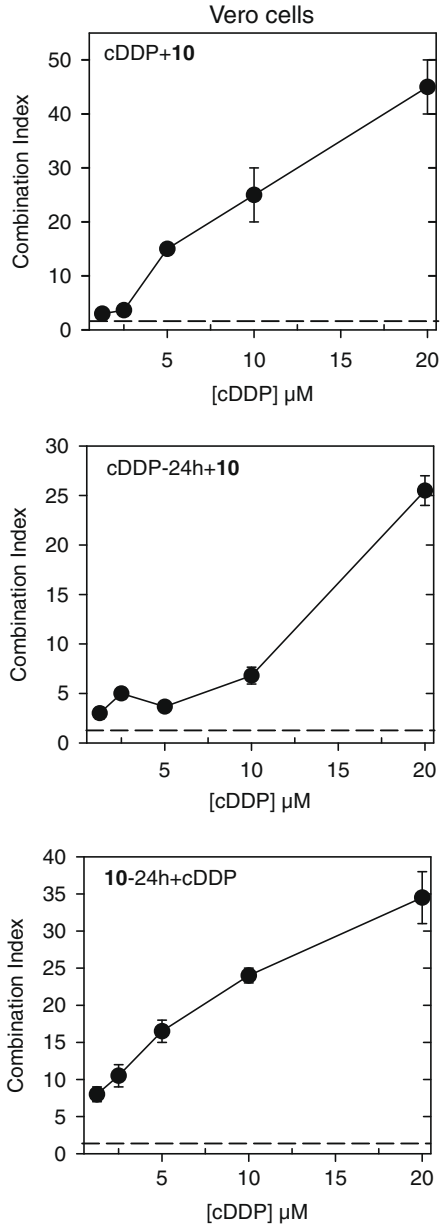

Figure 7. Median-effect analysis of cisplatin combined with compound **10** against Vero cells. Cells were allowed to attach overnight and then simultaneously (upper panel) or sequentially (middle and lower panel) treated with **10** and with the indicated concentrations of cDDP in 24-well plates. Following a 3-day exposure, cells were stained with crystal violet. Results are expressed as combination indexes (CI), where CI <1 indicate synergistic effects, CI >1 indicate antagonistic effects, CI = 1 indicate additivity. Results represent the mean of three separate experiments performed in duplicate. The standard error was within ±10% for each data point.

4.1.3. 1,7-Bis[3-methoxy-4-hydroxyphenyl]hepta-1,6-diene-3,5-dione (5); 1,7-bis[3-methoxy-4-acetylphenyl]hepta-1,6-diene-3,5-dione (6); 1,7-bis[4-(2,3,4,6-tetracetyl-β-d-glucopyranos-1-yloxy)phenyl]hepta-1,6-diene-3,5-dione (7); 1,7-bis[3-hydroxy-4-(2,3,4,6-tetracetyl-β-d-glucopyranos-1-yloxy)phenyl]hepta-1,6-diene-3,5-dione (8); 1,7-bis[3-methoxy-4-(2,3,4,6-tetracetyl-β-D-glucopyranos-1-yloxy)phenyl]hepta-1,6-diene-3,5-dione (9)

A suspension of 1.0×10^{-3} mol of B_2O_3 and 1.0×10^{-3} mol of acetylacetone in DMF (1.5 ml) was stirred for 30 min at 80 °C, followed by the addition of 4.0×10^{-3} mol of tributylborate. After 30 min 1.8×10^{-3} mol of the appropriate benzaldehyde was added. 0.4×10^{-3} mol of *n*-butylamine in 0.5 ml of DMF were slowly dropped (1 h). The solution kept under stirring at 80 °C for 4 h developed a yellow-orange colour. The solution was acidified with 8 ml of HCl 0.5 M. During the acidification, the solution was cooled to room temperature. The crude product initially appeared as heavy oil; but as stirring continued, it slowly transformed into an orange solid. After about 1 h of stirring, the solid was filtered and resuspended in water at room temperature. The crude solid was collected and dried in vacuum. Anal. Calcd for $C_{21}H_{20}O_6$ (**5**): C, 68.47; H, 5.47. Found: C, 68.41; H, 5.52, yield 60%; Anal. Calcd for $C_{25}H_{24}O_8$ (**6**): C, 66.36; H, 5.35. Found: C, 65.91; H, 5.73, yield 87%; Anal. Calcd for $C_{47}H_{60}O_{22}$ (**7**): C, 57.78; H, 6.19. Found: C, 58.57; H, 5.79, yield 81%; Anal. Calcd for $C_{47}H_{60}O_{24}$ (**8**): C, 55.95; H, 5.99. Found: C, 56.35; H, 6.07, yield 91%; Anal. Calcd for $C_{49}H_{64}O_{24}$ (**9**): C, 56.75; H, 6.22. Found: C, 57.09; H, 5.31, yield 77%. NMR chemical shifts (ppm in CD_3OD): (**5**) H-1 5.95, H-3 6.61, H-4 7.56, H-6 7.20, H-9 6.82, H-10 7.09; C-1 100.2, C-2 183.7, C-3 120.6, C-4 140.4, C-5 127.3, C-6 110.1, C-7 147.8, C-8 149.0, C-9 115.0, C-10 122.6; (**6**) H-1 5.94, H-3 6.59, H-4 7.57, H-6 7.49, H-7 6.82, H-9 6.82, H-10 7.49; C-1 100.3, C-2 183.6, C-3 120.4, C-4 140.2, C-5 126.5, C-6 129.3, C-7 115.3, C-8 160.1, C-9 115.3, C-10 129.3. NMR chemical shifts (ppm in $CDCl_3$): (**7**) H-1 5.80, H-3 6.52, H-4 7.61, H-6 7.00, H-7 7.50, H-9 7.50, H-10 7.00, H-11 5.14, H-12 5.29, H-13 5.28, H-14 5.18, H-15 3.89, H-16 4.29, H-16′ 4.18; C-1 99.5, C-2 180.7, C-3 120.7, C-4 125.9, C-5 133.2, C-6 135.2, C-7 114.7, C-8 162.3, C-9 114.7, C-10 135.2, C-11 96.3, C-12 68.2, C-13 70.7, C-14 66.0, C-15 69.1, C-16 58.9; (**8**) H-1 5.80, H-3 6.51, H-4 7.55, H-6 7.18, H-9 6.96, H-10 7.02, H-11 5.00, H-12 5.28, H-13 5.32, H-14 5.17, H-15 3.88, H-16 4.31, H-16′ 4.20; C-1 99.6, C-2 180.7, C-3 121.3, C-4 127.8, C-5 134.0, C-6 127.1, C-7 114.7, C-8 155.6, C-9 114.7, C-10 127.1, C-11 96.1, C-12 68.6, C-13 70.1, C-14 65.7, C-15 69.7, C-16 59.4; (**9**) H-1 5.82, H-3 6.51, H-4 7.58, H-6 7.10, H-9 7.04, H-10 7.05, H-11 5.02, H-12 5.27, H-13 5.28, H-14 5.16, H-15 3.80, H-16 4.26, H-16′ 4.17; C-1 99.1, C-2 180.6, C-3 120.9, C-4 137.5, C-5 129.1, C-6 109.2, C-7 148.3, C-8 145.2, C-9 117.1, C-10 119.1, C-11 99.7, C-12 68.6, C-13 70.0, C-14 65.8, C-15 69.6, C-16 59.4.

4.1.4. 1,7-Bis(4-β-d-glucopyranos-1-yloxophenyl)hepta-1,6-diene-3,5-dione (10); 1,7-bis(3-hydroxy-4-β-D-glucopyranos-1-yloxophenyl)hepta-1,6-diene-3,5-dione (11); 1,7-bis(3-methoxy-4-β-D-glucopyranos-1-yloxophenyl)hepta-1,6-diene-3,5-dione (12)

The acetylated compounds, solubilized in CH_3ONa 0.1 M methanolic solution, were kept under stirring for 2 h; pH was brought to neutrality by use of a DOWEX ion exchange resin, which was finally filtered off, and the solutions were evaporated under vacuum. Anal. Calcd for $C_{31}H_{36}O_{14}$ (**10**): C, 58.86; H, 5.74. Found: C, 56.50; H, 5.76. Anal. Calcd for $C_{31}H_{36}O_{16}$ (**11**): C, 56.02; H, 5.46. Found: C, 54.53; H, 6.79; Anal. Calcd for $C_{33}H_{40}O_{16}$ (**12**): C, 57.22; H, 5.82. Found: C, 53.83; H, 7.02.

NMR chemical shifts (ppm in CD_3OD): (**10**) H-1 6.01, H-3 6.69, H-4 7.62, H-6 7.14, H-7 7.61, H-9 7.60, H-10 7.14, H-11 4.98, H-12 3.52, H-13 3.47, H-14 3.42, H-15 3.45, H-16 3.91, H-16′ 3.71; C-1 102.8, C-2 185.6, C-3 124.5, C-4 142.1, C-5 131.6, C-6 131.6C-7 118.9, C-8 161.6, C-9 118.9, C-10 131.6, C-11 96.5, C-12 68.4, C-13 71.2, C-14 66.7, C-15 68,7, C-16 58.3; (**11**) H-1 6.01, H-3 6.63, H-4 7.53, H-6 7.14, H-9 7.20, H-10 7.07, H-11 4.97, H-12 3.53, H-13 3.47, H-14 3.44, H-15 3.45, H-16 3.90, H-16′ 3.71; C-1 102.8, C-2 185.4, C-3 124.5, C-4 142.1, C-5 132.6, C-6 116.2, C-7 147.7, C-8 149.4, C-9 118.8, C-10 122.8, C-11 96.3, C-12 68.1, C-13 71.4, C-14 65.0, C-15 70.1, C-16 59.2; (**12**) H-1 6.02, H-3 6.72, H-4 7.60, H-6 7.12, H-9 7.18, H-10 7.18, H-11 4.58, H-12 3.53, H-13 3.48, H-14 3.43, H-15 3.45, H-16 3.89, H-16′ 3.71; C-1 102.8, C-2 185.6, C-3 124.5, C-4 142.1, C-5 132.1, C-6 112.1, C-7 149.6,

C-8 150.1, C-9 117.3, C-10 122.5, C-11 99.4, C-12 68.1, C-13 70.5, C-14 66.2, C-15 69.7, C-16 59.2.

4.2. Spectroscopy

Spectrophotometric measurements were performed using Jasco V-570 spectrophotometer at 25 ± 0.1 °C in the 200–600 nm spectral range employing a 1 cm quartz cell. 2.5×10^{-5} M water solution of **10**, **11** and **12** were investigated; constant additions (10 μl) of $Ga(NO_3)_3$ solution (10^{-2} M) using a micropipette in order to reach different Me/L molar ratios.

NMR Spectra were recorded on a Bruker Avance AMX-400 spectrometer with a Broad Band 5 mm probe (inverse detection). Nominal frequencies are 100.13 MHz for ^{13}C and 400.13 MHz for ^{1}H. The typical acquisition parameters for ^{1}H are as follows: 20 ppm spectral bandwidth (SW), 6.1 μs pulse width (90° pulse hard pulse on ^{1}H), 0.5–1 s pulse delay, 216–512 number of scans. 0.5 ml of a CD_3OD 10^{-2} M solution of each ligand was prepared, then addition (10 μl) of $Ga(NO_3)_3$ (5×10^{-2} M in CD_3OD) was performed using a micropipette.

4.3. Kinetic studies

The chemical stability of the ligands was evaluated as a change in absorbance in the 385–440 nm range. The aqueous solutions of the ligands, concentration from 1×10^{-5} to 5×10^{-5} M ,were prepared in 10^{-2} M phosphate buffered solution (pH 7). A constant ionic strength of 0.1 M ($NaNO_3$) was maintained in all experiments. The cell was stored at 37 °C. The spectra were recorded every 30 min for 8 h.

4.4. Cell lines

The 2008 cell line, established from a patient with serous cystadenocarcinoma of the ovary and the cDDP-resistant C13* subline, generated as previously described,[36] were grown as monolayers in RPMI 1640 medium (BioWhittaker Europe) containing 10% heat-inactivated fetal bovine serum (BioWhittaker Europe) and 50 μg/ml gentamycin sulfate. Cultures were equilibrated with humidified 5% CO_2 in air at 37 °C. All studies were performed in *Mycoplasma* negative cells, as routinely determined with the *Mycotest* detection kit (Euroclone, Switzerland).

Vero cells, established from kidney cells of the African green monkey (*Cercopithecus aethiops*), were chosen as a control cell line[18] These cells were obtained from the Istituto Zooprofilattico (Brescia, Italy), and maintained in MEM medium (Whittaker Bioproducts, Walkersville, MD, USA) supplemented with 10% heat-inactivated fetal calf serum (Gibco/BRL, Gaithersburg, MD, USA) and penicillin G (100 μg/ml), streptomycin (100 μg/ml) (Sigma Chemical Company, MO, USA). Cultures were equilibrated with humidified 5% CO_2 in air at 37 °C. The medium was renewed at 48 h intervals, and the cells were always subcultured when the monolayers become confluent.

4.5. Cytotoxicity assay

Cell growth in the absence or in the presence of the compounds was assessed by a modification of the crystal violet dye assay.[37] Cells were seeded at a density of 4×10^4 cells/well of a 24-well culture plate (Sarstedt, Numbrecht, Germany) and cultured for 72 h at 37 °C (control cells). Treated cells were incubated with different concentrations of the compounds and were grown under the same conditions as non-treated (control) cells. After incubation, the culture medium was removed and the cells were washed with 0.1 ml of 0.1 M phosphate-buffered saline (PBS), pH 7.4 at 37 °C, then cell monolayer was fixed with methanol prior to staining with 0.1% crystal violet solution in 80% absolute ethanol for at least 30 min. After washing several times with distilled water to remove the dye excess, the cells were let to dry. The incorporated dye was solubilized in acidic isopropanol (1 N HCl/2-propanol, 1:10). After appropriate dilution, dye was determined spectrophotometrically at 540 nm. The extracted dye was proportional to cell number. Percentage of cytotoxicity was calculated by comparing the absorbance of exposed to non-exposed (control) cultures.

4.6. Median-effect analysis

Median-effect analysis was used to determine the nature of the combination between cisplatin and compound **10** combined at a fixed ratio.[34] Computer analysis by Calcusyn software, Biosoft, Cambridge, UK) of the dose–response curves was used to calculate the combination index (CI) at increasing levels of cell kill. CI values of less than or greater than 1 indicate synergy and antagonism, respectively, whereas a CI value of 1 indicates additivity of the drugs.

Acknowledgement

We are thankful to 'Centro Interdipartimentale Grandi Strumenti (CIGS)' of the University of Modena and Reggio Emilia, which supplied NMR Spectrometer.

References and notes

1. Wong, E.; Giandomenico, C. M. *Chem. Rev.* **1999**, *99*, 2451.
2. Kelland, L. R. *Drugs* **2000**, *59*, 1.
3. Hatchera, H.; Planalpb, R.; Chob, J.; Tortia, F. M. *Cell. Mol. Life Sci.* **2008**, *65*, 1631.
4. Adams, B. K.; Ferstl, E. M.; Davis, M. C.; Herold, M.; Kurtkaya, S.; Camalier, R. F.; Hollingshead, M. G.; Kaur, G.; Sausville, E. A.; Rickles, F. R.; Snyder, J. P.; Liotta, D. C.; Shoji, M. *Bioorg. Med. Chem.* **2004**, *12*, 3871.
5. Weir, N. M.; Selvendiran, K.; Kutala, V. K.; Tong, L.; Vishwanath, S.; Rajaram, M.; Tridandapani, S.; Anant, S.; Kuppusamy, P. *Cancer Biol. Ther.* **2007**, *6*, 178.
6. John, V. D.; Kuttan, G.; Krishnankutty, K. *J. Exp. Clin. Cancer Res.* **2002**, *21*, 219.
7. Shen, L.; Ji, H. F. *Spectrochim. Acta, Part A* **2007**, *67*, 619.
8. Borsari, M.; Ferrari, E.; Grandi, R.; Saladini, M. *Inorg. Chim. Acta* **2002**, *328*, 61.
9. Jiao, Y.; Wilkinson, J., IV; Pietsch, E. C.; Buss, J. L.; Wang, W.; Planalp, R.; Torti, F. M.; Torti, S. V. *Free Radical Biol. Med.* **2006**, *40*, 1152.
10. Bussl, J. L.; Torti, F. M.; Torti, S. V. *Curr. Med. Chem.* **2003**, *10*, 1021.
11. Anand, P.; Kunnumakkara, A. B.; Newman, R. A.; Aggarwal, B. B. *Mol. Pharmaceutics* **2007**, *4*, 807.
12. Kumar, S.; Narain, U.; Tripathi, S.; Misra, K. *Bioconjugate Chem.* **2001**, *12*, 464.
13. Shi, W.; Dolai, S.; Rizk, S.; Hussain, A.; Tariq, H.; Averick, S.; L'Amoreaux, W.; El Idrissi, A.; Banerjee, P.; Raja, K. *Org. Lett.* **2007**, *9*, 5461.
14. Safavy, A.; Raisch, K. P.; Mantena, S.; Sanford, L. L.; Sham, S. W.; Rama Krishna, N.; Bonner, J. A. *J. Med. Chem.* **2007**, *50*, 6284.
15. Bianchi, N. O.; Ayres, J. *Exp. Cell. Res.* **1971**, *68*, 253.
16. Santos, A. R., Jr.; Dolder, H.; Wada, M. L. F. *J. Submicrosc. Cytol. Pathol.* **2003**, *35*, 35.
17. Zhang, M.; Bian, F.; Wen, C.; Hao, N. *J. Huazhong Univ. Sci. Technol. Med. Sci.* **2007**, *27*, 339.
18. Menezo, Y. J. R.; Guerin, J. F.; Czyba, J. C. *Biol. Reprod.* **1990**, *42*, 301.
19. Rossi, T.; Coppi, A.; Bruni, E.; Ruberto, A.; Santachiara, S.; Baggio, G. *Anticancer Res.* **2007**, *27*, 2555.
20. Mishra, S.; Narain, U.; Mishra, R.; Misra, K. *Bioorg. Med. Chem.* **2005**, *13*, 1477.
21. Pabon, H. J. J. *Rec. Trav. Chim.* **1964**, *83*, 379.
22. Buss, J. L.; Torti, F. M.; Torti, S. V. *Curr. Med. Chem.* **2003**, *10*, 1021.
23. Solčániova, E.; Hrnčiar, P.; Liptaj, T. *Org. Magn. Res.* **1982**, *18*, 55.
24. Arrieta, A. F.; Mostad, A. *Acta Crystallogr., Sect. E* **2001**, *57*, o1198.
25. Atkinson, R. A.; Salah El Din, A. L.; Kieffer, B.; Lefevre, J. F.; Abdallah, M. A. *Biochemistry* **1998**, *37*, 15965.
26. Hara, Y.; Shen, L.; Tsubouchi, A.; Akiyama, M.; Umemoto, K. *Inorg. Chem.* **2000**, *39*, 5074.
27. Hegetschweiler, K.; Kradolfer, T.; Gramlich, V.; Hancock, R. D. *Chem. Eur. J.* **1995**, *1*, 74.
28. Hegetschweiler, K.; Hausherr-Primo, L.; Koppenol, W. H.; Gramlich, V.; Odier, L.; Meyer, W.; Winkler, H.; Trautwein, A. X. *Angew. Chem., Int. Ed. Engl.* **1995**, *34*, 2242.
29. Hegetschweiler, K.; Ghisletta, M.; Hausherr-Primo, L.; Kradolfer, T.; Schmalle, H. W.; Gramlich, V. *Inorg. Chem.* **1995**, *34*, 1950.
30. Wang, Y. J.; Pan, M. H.; Cheng, A. L.; Lin, L. I.; Ho, Y. S.; Hsieh, C. Y.; Lin, J. K. *J. Pharm. Biomed. Anal.* **1997**, *15*, 1867.
31. Tomren, M. A.; Másson, M.; Loftsson, T.; Tønnensen, H. H. *Int. J. Pharm.* **2007**, *338*, 27–34.

32. Adams, B. K.; Ferstl, E. M.; Davis, M. C.; Herold, M.; Kurtkaya, S.; Camalier, R. F.; Hollingshead, M. G.; Kaur, G.; Sausville, E. A.; Rickles, F. R.; Snyder, J. P.; Liotta, D. C.; Shoji, M. *Bioorg. Med. Chem.* **2004**, *12*, 3871–3883.
33. Kuhar, M.; Imran, S.; Singh, N. *J. Cancer Mol.* **2007**, *3*, 121–128.
34. Chou, T. C.; Talalay, P. *Adv. Enzyme Regul.* **1984**, 27–55.
35. Fischer, E. *Chem. Ber.* **1911**, *44*, 1898–1904.
36. Andrews, P. A.; Albright, K. D. *Cancer Res.* **1992**, *52*, 1895–1901.
37. Kueng, W.; Siber, E.; Eppenberger, U. *Anal. Biochem.* **1989**, *182*, 16.